

# Mechanism of a Cobalt(III)-Catalyzed Olefin Hydrosilation Reaction: Direct Evidence for a Silyl Migration Pathway

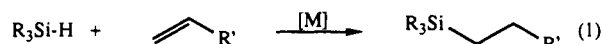
M. Brookhart\* and B. E. Grant

Contribution from the Department of Chemistry, The University of North Carolina, Chapel Hill, North Carolina 27599-3290. Received August 27, 1992

**Abstract:** The electrophilic Co(III) complex  $[\text{Cp}^*(\text{P}(\text{OMe})_3)\text{CoCH}_2\text{CH}_2-\mu\text{-H}]^+ \text{BAR}'_4^-$  (**1**;  $\text{BAR}'_4^- = \text{B}[3,5-(\text{CF}_3)_2\text{C}_6\text{H}_3]_4^-$ ) has been demonstrated to be an efficient catalyst for the regiospecific hydrosilation of 1-hexene. The spectroscopic detection of the catalyst resting state species  $[\text{Cp}^*(\text{P}(\text{OMe})_3)\text{CoCH}(\text{Bu})\text{CH}(\text{SiEt}_3)-\mu\text{-H}]^+$  (**2**) in solutions of working catalyst systems has provided direct evidence for a silyl migration pathway. The spectroscopic detection of  $[\text{Cp}^*(\text{P}(\text{OMe})_3)\text{CoCH}_2\text{CH}-\{(\text{CH}_2)_4\text{SiEt}_3\}-\mu\text{-H}]^+$  (**6**), along with supporting kinetics and deuterium labeling experiments, established the turnover-limiting step as the isomerization of **2** to **6**.

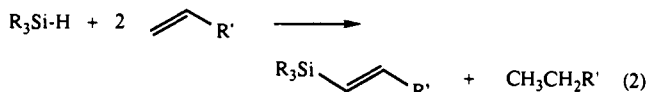
## Introduction

Transition metal catalyzed hydrosilation of olefins is an important reaction for the formation of silicon-carbon bonds (eq 1).<sup>1</sup> A widely accepted mechanism for this process was first proposed by Chalk and Harrod.<sup>2</sup> As Figure 1 illustrates, the key



feature of this mechanism is hydride migratory insertion. As well as providing a mechanism for product formation, this pathway also accounts for a number of observations associated with hydrosilation catalysis, namely, deuterium scrambling and olefin isomerization. Classical reversible  $\beta$ -hydride elimination and readdition sequences from the alkylsilyl intermediate accommodate these observations.<sup>3</sup>

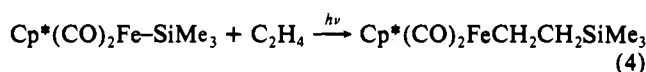
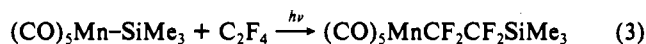
A number of hydrosilation catalysts form vinylsilanes and alkanes along with hydrosilation product as illustrated in eq 2.<sup>4-8</sup> The classical Chalk-Harrod mechanism does not account for these products, prompting a number of groups to propose silyl migration as an integral or competing step in the hydrosilation pathway.<sup>4-8</sup>



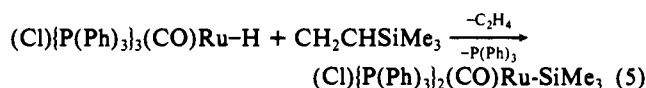
One such pathway that parallels the Chalk-Harrod cycle is shown in Figure 2. Here, silyl migratory insertion results in a  $\beta$ -silylalkyl hydride intermediate, which can then undergo two possible reactions. Reductive elimination gives the hydrosilation product, while  $\beta$ -hydride elimination forms vinylsilane and a metal dihydride species that is responsible for hydrogenation of olefin. It

has been noted that silyl migration mechanisms such as this do not require silylalkyl reductive elimination, the one step in the Chalk-Harrod cycle for which little precedent exists.<sup>9</sup>

Apart from the formation of vinylsilanes during hydrosilation catalysis, a limited amount of other evidence supporting silyl migratory insertion reactions has been accumulated. The isolation of  $\beta$ -silylalkyl complexes resulting from olefin insertion into metal-silicon bonds has been accomplished (eqs 3<sup>10</sup> and 4<sup>11</sup>), providing the most direct evidence, albeit in stoichiometric rather than catalytic reactions. The reverse of this process,  $\beta$ -silyl



elimination, has also been established, as the formation of the Ru-silyl complex in eq 5 clearly shows.<sup>12</sup>



Direct evidence for silyl migration during hydrosilation catalysis is limited. Control experiments by Wrighton established that  $(\text{CO})_4\text{Co-SiMe}_3$ , an effective hydrosilation catalyst, will undergo olefin insertion into the Co-Si bond upon photolysis of the complex under ethylene.<sup>13</sup> Recent reports by Perutz<sup>14</sup> and Bosnich<sup>15</sup> demonstrated, through deuterium labeling techniques, that silyl migration mechanisms were operative in hydrosilation pathways. Noticeably absent, however, has been the detection and characterization of key intermediates in hydrosilation cycles. Efforts to detect intermediates (and thereby gain mechanistic information) have been hampered by inconveniently high catalytic rates<sup>15</sup> and heterogeneous systems.<sup>16</sup> Moreover, the identification of resting-state structures in hydrosilation catalytic systems does not necessarily distinguish between hydride and silyl migration pathways. Perutz, for example, identified  $\text{CpRh}(\text{C}_2\text{H}_4)(\text{H})(\text{SiR}_3)$

(1) (a) Harrod, J. F.; Chalk, A. J. In *Organic Synthesis via Metal Carbonyls*; Wender, I., Pino, P., Eds.; Wiley: New York, 1977; Vol. 2. (b) Speier, J. L. *Adv. Organomet. Chem.* **1979**, *17*, 407. (c) Ojima, I. In *The Chemistry of Organic Silicon Compounds*; Patai, S., Rappoport, Z., Eds.; Wiley: New York, 1989.

(2) (a) Chalk, A. J.; Harrod, J. F. *J. Am. Chem. Soc.* **1965**, *87*, 16. (b) Chalk, A. J.; Harrod, J. F. *J. Am. Chem. Soc.* **1965**, *87*, 1183.

(3) Collman, J. P.; Hegedus, L. S.; Norton, J. R.; Fink, R. G. *Principles and Applications of Organotransition Metal Chemistry*; University Science Books: Mill Valley, CA, 1987.

(4) (a) Mitchener, J. C.; Wrighton, M. S. *J. Am. Chem. Soc.* **1981**, *103*, 975. (b) Schroeder, M. A.; Wrighton, M. S. *J. Organomet. Chem.* **1977**, *128*, 345.

(5) (a) Millan, A.; Fernandez, M.-J.; Bentz, P.; Maitlis, P. *J. Mol. Catal.* **1984**, *26*, 89. (b) Milan, A.; Towns, E.; Maitlis, P. M. *J. Chem. Soc., Chem. Commun.* **1981**, 673.

(6) (a) Seki, Y.; Takeshita, K.; Kawamoto, K. *J. Organomet. Chem.* **1989**, *369*, 117. (b) Seki, Y.; Takeshita, K.; Kawamoto, K.; Murai, S.; Sonoda, N. *J. Org. Chem.* **1987**, *52*, 4864.

(7) (a) Onopchenko, A.; Sabourin, E. T.; Beach, D. L. *J. Org. Chem.* **1984**, *49*, 3389. (b) Onopchenko, A.; Sabourin, E. T.; Beach, D. L. *J. Org. Chem.* **1983**, *48*, 5101.

(8) Ojima, I.; Fuchikami, T.; Yatabe, M. *J. Organomet. Chem.* **1984**, *260*, 335.

(9) (a) Brinkman, K. C.; Blakeney, A. J.; Krone-Schmidt, W.; Gladzy, J. A. *Organometallics* **1984**, *3*, 1325. (b) Blakeney, A. J.; Gladzy, J. A. *Inorg. Chim. Acta* **1980**, *53*, L25.

(10) Clark, H. C.; Hauw, T. L. *J. Organomet. Chem.* **1972**, *42*, 429. (11) Randolph, C. L.; Wrighton, M. S. *J. Am. Chem. Soc.* **1986**, *108*, 3766. See also: Arnold, J.; Engeler, M. P.; Eisner, F. H.; Heyn, R. H.; Tilley, T. D. *Organometallics* **1989**, *8*, 2284.

(12) Wakatsuki, Y.; Yamazaki, H.; Nakano, M.; Yamamoto, Y. *J. Chem. Soc., Chem. Commun.* **1991**, 703.  $\beta$ -silyl elimination was also noted in refs 6a and 11.

(13) Seitz, F.; Wrighton, M. S. *Angew. Chem., Int. Ed. Engl.* **1988**, *27*, 289.

(14) Duckett, S. B.; Perutz, R. N. *Organometallics* **1992**, *11*, 90.

(15) See, for example: Bergens, S. H.; Noheda, P.; Whelan, J.; Bosnich, B. *J. Am. Chem. Soc.* **1992**, *114*, 2128.

(16) Lewis, L. N. *J. Am. Chem. Soc.* **1990**, *112*, 5998.

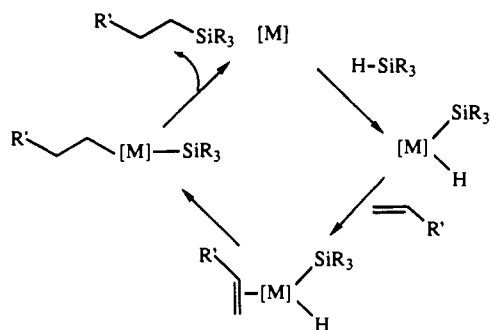
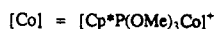
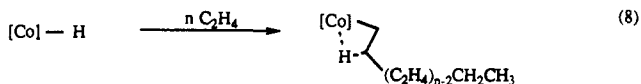
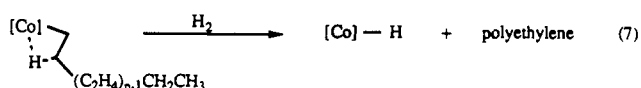
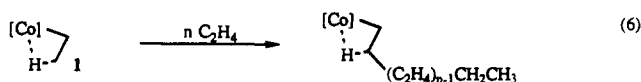


Figure 1. Chalk-Harrod mechanism for olefin hydrosilylation.

as the resting-state structure in a Rh(III)-catalyzed hydrosilylation system, a complex whose ligand array is common to both the Chalk-Harrod and silyl migration pathways shown in Figures 1 and 2.<sup>14</sup>

Our interest in hydrosilylation began from ongoing investigations of olefin polymerization and oligomerization reactions catalyzed by electrophilic Co(III) complexes.  $[\text{Cp}^*(\text{P}(\text{OMe})_3)\text{CoCH}_2\text{CH}_2-\mu\text{-H}]^+ \text{BAR}'_4^-$  (**1**), which is formed by the protonation of  $\text{Cp}^*(\text{P}(\text{OMe})_3)\text{Co}(\text{CH}_2\text{CH}_2)$  with  $\text{HBAR}'_4(\text{Et}_2\text{O})_2$  ( $\text{Ar}' = 3,5\text{-}(\text{CF}_3)_2\text{C}_6\text{H}_3$ ),<sup>17</sup> serves as an effective ethylene polymerization catalyst.<sup>18</sup> Hydrogenolysis of the metal-bound polymer chain led to clean polymer recovery and to the formation of a cobalt hydride species. Exposure of this complex to ethylene led to further polymerization (eqs 6-8).<sup>19</sup>



This reaction sequence suggested that **1** may function as an olefin hydrogenation catalyst. Preliminary results supported this contention, as it was shown that under a hydrogen atmosphere **1** catalyzed the efficient hydrogenation of 1-hexene.<sup>19</sup> As Figure 3 indicates, a plausible mechanism involves hydride migration to the coordinated olefin to form a bridging agostic intermediate, the structure that  $\beta$ -alkyl-substituted analogues of **1** are known to adopt.<sup>20</sup>

Drawing parallels between  $\text{H}_2$  and  $\text{R}_3\text{SiH}$ , we reasoned that **1** may also be a viable hydrosilylation catalyst. We report here that, indeed, **1** serves as an entry into an efficient system for the catalytic hydrosilylation of 1-hexene. Furthermore, two key intermediates in the catalytic cycle have been identified that, coupled with kinetics and deuterium labeling experiments, have allowed elucidation of the hydrosilylation mechanism.

## Results and Discussion

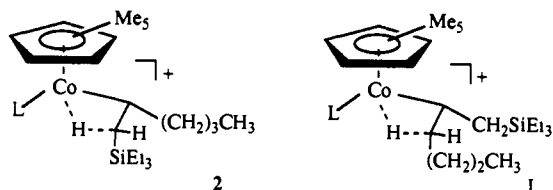
**A. General.** To test the viability of **1** as a hydrosilylation catalyst, a  $\text{CH}_2\text{Cl}_2$  solution of **1** was treated with 100 equiv each of  $\text{Et}_3\text{SiH}$  and 1-hexene. After 6 h both reagents had been consumed, and  $\text{Et}_3\text{Si}(\text{CH}_2)_5\text{CH}_3$  was recovered as the exclusive product in a 75%

isolated yield (ca. 95% GC yield), with no evidence for the formation of the 2-silyl regioisomer (<1% by  $^{13}\text{C}$  NMR analysis). A small amount (ca. 5% by  $^{13}\text{C}$  NMR analysis) of  $(\text{Et}_3\text{Si})_2\text{O}$  was also observed. It was found by monitoring the reaction by GC that  $\text{Et}_3\text{Si}(\text{CH}_2)_5\text{CH}_3$  forms cleanly in yields that approach 100% for up to ca. 200 turnovers with an initial turnover rate of  $0.5 \text{ min}^{-1}$ . A maximum of 300-400 turnovers can be achieved before the reaction stops due to gradual catalyst decomposition.

Having established that **1** regioselectively catalyzes the hydrosilylation of 1-hexene, we sought mechanistic information. The 15-electron  $[\text{Cp}^*(\text{P}(\text{OMe})_3)\text{Co}]^+$  fragment lacks the necessary coordination sites to accommodate both silane and olefin ligands; Chalk-Harrod type pathways that involve intermediates which bind both silane and olefin to the intact  $[\text{Cp}^*(\text{P}(\text{OMe})_3)\text{Co}]^+$  unit were therefore considered unlikely. As shown in Figure 4, two plausible pathways begin with silane-induced Co-alkyl cleavage leading to either Co-H or Co-SiEt<sub>3</sub> intermediates and entry into a catalytic cycle. Pathway A features silyl migratory insertion as the key step, while pathway B involves hydride migration.

**B. NMR Studies of Intermediates.** Variable temperature  $^1\text{H}$  NMR spectra of working catalyst solutions were obtained in order to detect intermediates. Addition of 5 equiv of each reagent to a  $\text{CD}_2\text{Cl}_2$  solution of **1** at 25 °C followed by quick cooling of the sample to -70 °C revealed ethane ( $\delta = 0.80 \text{ ppm}$ ) and two upfield signals, in a 1:1 ratio, at -1.5 and -9.8 ppm. In a separate experiment, an excess of 1-hexene was used and the progress of the hydrosilylation reaction was monitored at 0 °C by observing the disappearance of  $\text{Et}_3\text{SiH}$  signals; at this temperature, the upfield signals at -1.5 and -9.8 ppm remained prominent until silane was depleted. When silane was depleted, the peaks at -1.5 and -9.8 ppm greatly diminished in intensity, and upon cooling of the sample to -70 °C, a new set of upfield signals was observed. The new signals at -13.2, -12.9, and -11.9 ppm broadened considerably at temperature above -50 °C.

The formation of ethane at early stages in the catalysis suggested that pathway A in Figure 4 was operative. In this mechanism, silyl migration to coordinated hexene is required, and the  $\beta$ -silylalkyl-cobalt intermediate so formed is assigned structure **2** on the basis of its  $^1\text{H}$  NMR properties. Specifically, the initially



observed upfield signals at -9.5 and -1.5 ppm correspond to  $\mu\text{-H}$  and  $\beta\text{-H}$ , respectively, of **2**, in which a Si-C-H bridge and not a C-C-H bridge (as in alternative structure **1**) is present. The  $\beta\text{-H}$  in analogous  $\beta$ -alkyl-substituted agostic complexes typically resonates at 0-1.5 ppm; the relatively high field shift of the  $\beta\text{-H}$  in **2** is thus consistent with a  $\beta$ -silyl- rather than a  $\beta$ -alkyl-substituted agostic structure. The well-resolved ddd pattern exhibited by the  $\beta\text{-H}$  signal likewise supports structure **2**, whereas a more complicated coupling would be anticipated for the  $\beta\text{-H}$  in **1**.

The identification of **2** as the catalyst resting state was also made on the basis of its variable temperature  $^1\text{H}$  NMR features. In analogous  $\beta$ -alkyl-substituted Co(III) compounds, rotation about the  $\text{C}_\alpha\text{-C}_\beta$  bond is a relatively low energy process; two rotamers are observed at -80 °C, and broadening of the  $\beta\text{-H}$  and  $\mu\text{-H}$  signals of these rotamers as the result of rotation around the  $\text{C}_\alpha\text{-C}_\beta$  bond occurs at temperatures  $> -50$  °C.<sup>20</sup> Only a single isomer of **2** is observed, however. Presumably because of the steric congestion that would arise if  $\text{SiEt}_3$  were directed toward the  $\text{Cp}^*$  ligand, the rotamer in which the  $\text{SiEt}_3$  is directed away from the  $\text{Cp}^*$  is strongly favored and, thus,  $\beta\text{-H}$  and  $\mu\text{-H}$  signals remain sharp and well-resolved up to 0 °C. Complex **2** is the first example of an  $\alpha,\beta$ -disubstituted agostic complex belonging to the general formula  $[\text{C}_5\text{R}_5(\text{L})\text{CoR}]^+$ . A syn arrangement of the butyl and silyl groups has been assigned, again on the basis of steric considerations whereby the  $\alpha$ -alkyl is also directed away from the  $\text{Cp}^*$  ligand.

(17) Brookhart, M.; Grant, B.; Volpe, A. F., Jr. *Organometallics* 1992, 11, 3920. The synthesis of the analogous  $\text{BF}_4^-$  salt has been described; see refs 18 and 20.

(18) (a) Schmidt, G. F.; Brookhart, M. *J. Am. Chem. Soc.* 1985, 107, 1443. (b) Brookhart, M.; Volpe, A. F., Jr.; Lincoln, D. M.; Horváth, I. T.; Millar, J. M. *J. Am. Chem. Soc.* 1990, 112, 5634.

(19) Brookhart, M.; Volpe, A. F., Jr. Unpublished results.

(20) Brookhart, M.; Lincoln, D. M.; Volpe, A. F., Jr.; Schmidt, G. F. *Organometallics* 1989, 8, 1212.

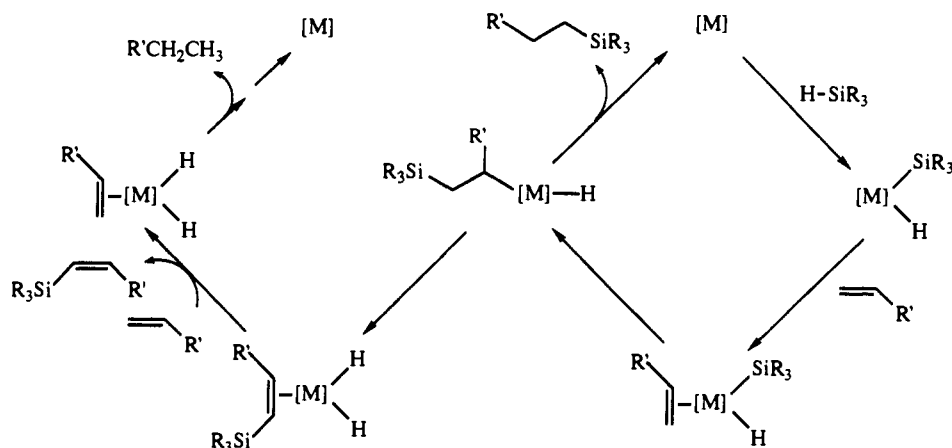


Figure 2. Hydrosilation and vinylsilane formation by a silyl migration pathway.

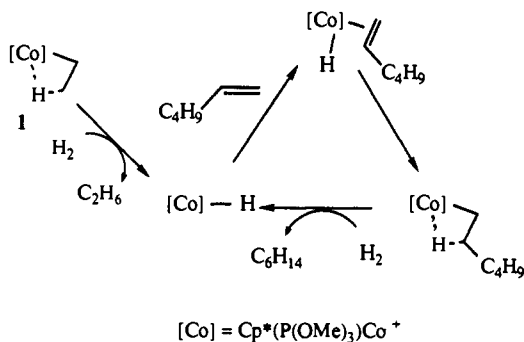


Figure 3. Hydrogenation of 1-hexene catalyzed by complex 1.

Confirmation of intermediate **2** came from the preparation and characterization of structural analogues. Substitution of trialkylvinylsilanes for propene in complex **3** gave the corresponding vinylsilane complexes **4** (eq 9). Protonation of **4** generated the

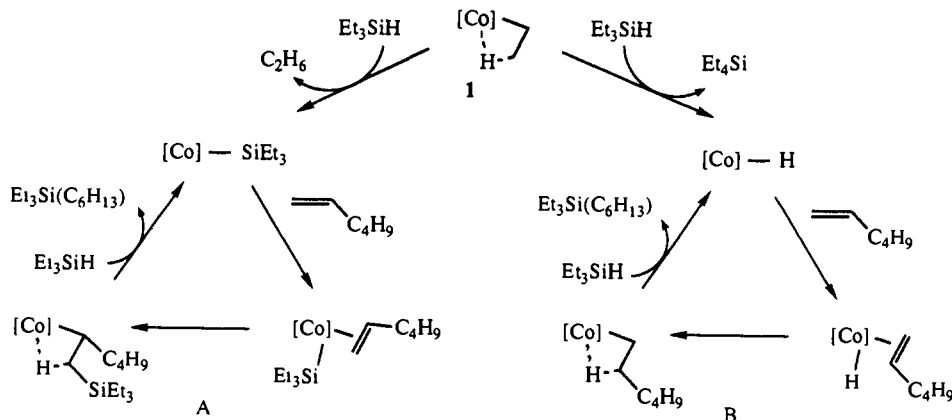
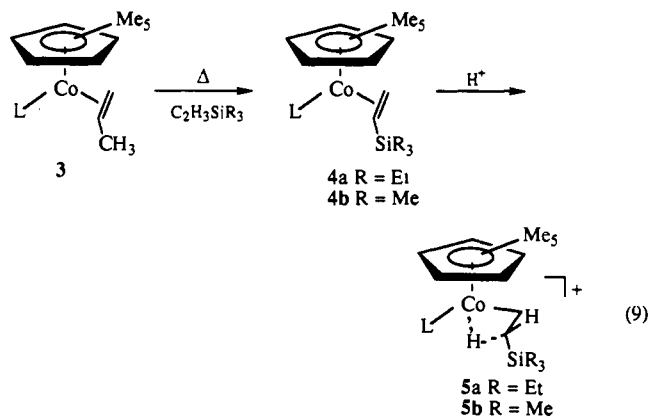


Figure 4. Possible pathways for hydrosilation of 1-hexene catalyzed by complex 1.

Table I. Dependence of Turnover Rates on 1-Hexene and Et<sub>3</sub>SiH Concentrations

[1] (M) <sup>a</sup>	Et <sub>3</sub> SiH (equiv)	1-hexene (equiv)	turnover rate (min <sup>-1</sup> ) <sup>b</sup>
0.01	50	100	0.49 ± 0.01
0.01	100	100	0.54 ± 0.02
0.01	250	100	0.51 ± 0.02
0.01	50	50	0.51 ± 0.01
0.01	50	250	0.50 ± 0.01

<sup>a</sup> C<sub>6</sub>H<sub>5</sub>Cl solution, 20 °C. <sup>b</sup> Initial turnover rate as determined after ca. 12 turnovers, monitored by GC using dodecane as internal standard, with error margins = 1 SD of the slope of turnover rate plots.

highly electrophilic salts **5**, which, because of their highly electrophilic nature, could not be isolated in pure form. Both **5a** and (especially) **5b** readily decompose to give (Et<sub>3</sub>Si)<sub>2</sub>O and **1**, whose formation we attribute to reaction with traces of water. (In a similar fashion, attack by traces of water on intermediate **2** leads to the formation of (Et<sub>3</sub>Si)<sub>2</sub>O during catalysis.) In an alternative approach to generate **5**, the catalytic hydrogenation of R<sub>3</sub>Si(CH=CH<sub>2</sub>) was carried out. It was reasoned that **5** would be the resting-state structure for this process, as a result of insertion of R<sub>3</sub>Si(CH=CH<sub>2</sub>) into Cp\*[P(OMe)<sub>3</sub>]CoH<sup>+</sup>. It was hoped that after sufficient turnovers all traces of moisture would be consumed, and **5** could be observed free from **1**. While **5** still resisted isolation, this method did provide a means of generating relatively clean solutions of **5** for <sup>1</sup>H NMR study.

Spectroscopic features of **5** are similar to those of **2** and support the structural assignments made. Specifically, complex **5a** exhibited <sup>1</sup>H NMR signals at -10.4 and -1.6 ppm which did not broaden significantly until 0 °C. These correspond to μ-H and β-H, respectively. <sup>13</sup>C NMR spectroscopy revealed a signal at -24.4 ppm with a reduced *J*(C<sub>β</sub>-H) value of 74 Hz in **5a**, confirming the presence of an agostic interaction in this species and, by analogy, in catalytic intermediate **2**. Broadening of signals

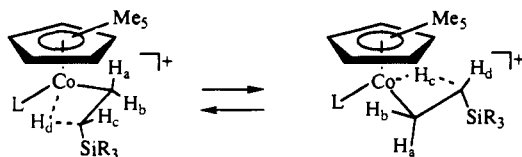
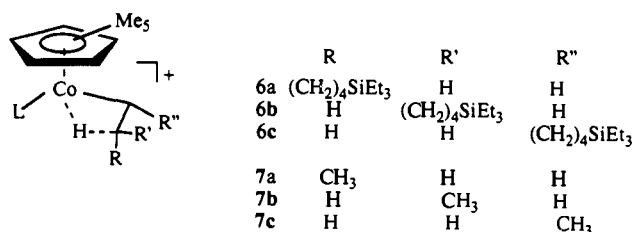


Figure 5. Inversion at Co in complex 6.

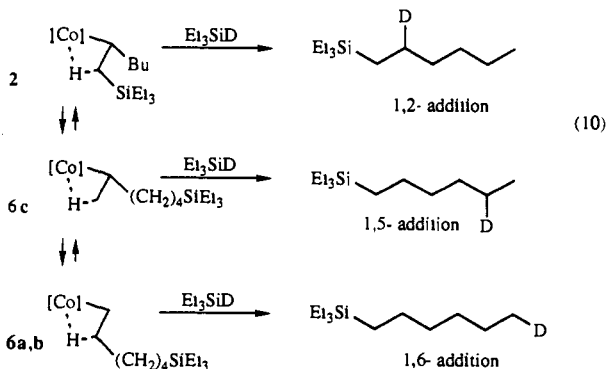
from  $\mu$ -H,  $\beta$ -H, and  $\alpha$ -H at room temperature, with the maintenance of sharp Cp\* and P(OMe)<sub>3</sub> signals, indicated that a signal degenerate fluxional process occurs. It is proposed that this process corresponds to inversion at cobalt as shown in Figure 5. Analogous behavior has been observed in  $\beta$ -alkyl analogs of **5**.<sup>20,21</sup>

According to pathway A, the reaction of **2** with Et<sub>3</sub>SiH results in hydrosilation product formation and completion of the catalytic cycle. It remained, however, to account for the three new hydride resonances that appeared when the catalytic system was allowed to become depleted in Et<sub>3</sub>SiH. The chemical shift, multiplicities, and variable temperature behavior of these signals were clearly indicative of an equilibrium mixture of isomeric, alkyl-substituted agostic species (**6a-c**). Again, structure assignment was based



on close analogy. Protonation of Cp\*(P(OMe)<sub>3</sub>)Co(CH<sub>2</sub>CHCH<sub>3</sub>) yields a comparable set of well-characterized alkyl-substituted complexes (**7a-c**).<sup>20</sup> This set of isomers exhibits a nearly identical pattern in the upfield region of the <sup>1</sup>H NMR spectrum (-11.8 to -13.2 ppm). As further support for structures **6a-c**, the dynamic behavior as measured by the temperature-dependent line broadening in the upfield region also closely matches the temperature-dependent behavior of the upfield signals of **7a-c**. The formation of complexes **6a-c** from **2** results from a series of  $\beta$ -elimination/migratory insertion steps.

**C. Deuterium Labeling Studies.** It was unclear initially if the isomeric complexes **6a-c**, which appeared only when silane was depleted, were involved directly in the catalytic pathway. Conceivably, complexes **2** or **6a-c** (or other secondary alkyl-Co species which must be involved in the conversion of **2** to **6**) could react with Et<sub>3</sub>SiH to form the hydrosilation product and complete the cycle. To determine which reaction (or combination of reactions) occurred during catalysis, a deuterium labeling study was carried out using Et<sub>3</sub>SiD. As shown in eq 10, "1,2-" and "1,6-deutero-



silation" were two possible outcomes of this experiment and would implicate complexes **2** and **6a,b**, respectively, as the reactive species toward silane. Furthermore, the possibility that complex **2** was

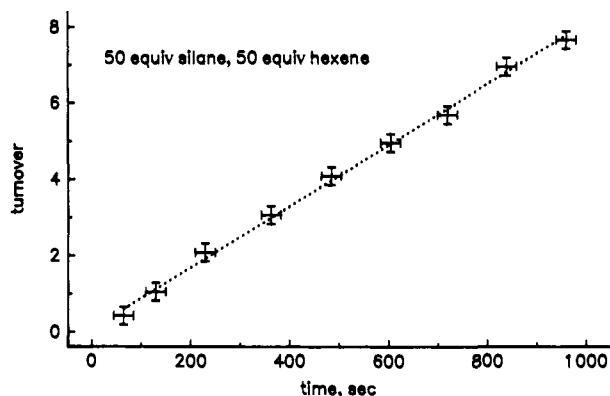


Figure 6. Representative initial turnover rate plot for the catalytic hydrosilation of 1-hexene using **[1]** = 0.01 M and **[Et<sub>3</sub>SiH]** = 1-hexene concentration = 0.50 M.

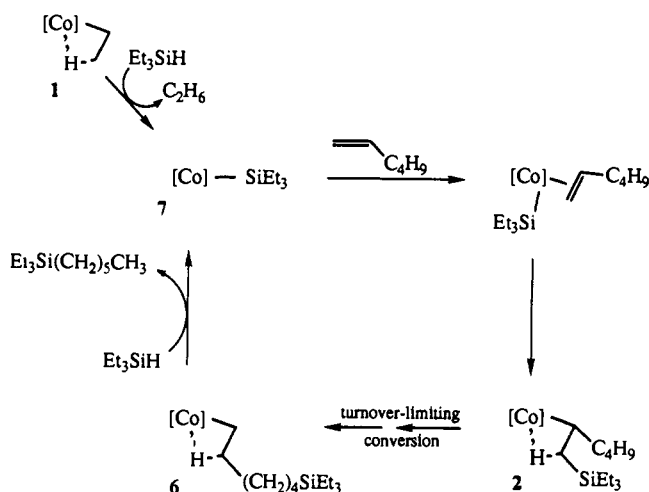


Figure 7. Overall pathway for the catalytic hydrosilation of 1-hexene.

the branch point for two viable pathways, whose occurrences were dependent on silane concentration, was considered. Thus, it was plausible that at high silane concentrations trapping of complex **2** and the resultant formation of the 1,2-addition product would occur, while at relatively low silane concentrations the rate of this step would diminish to the point that the isomerization of **2** (whose rate is independent of silane concentration) would predominate and the product of 1,6-addition would be observed. Catalytic runs using 10 and 100 equiv of Et<sub>3</sub>SiD were allowed to react for 12 h. The hydrosilation product from both runs and that from a sample taken from the 100-equiv run that was quenched after a 10-min reaction time (ca. 5 turnovers, i.e., reflecting conditions of high silane concentration) were each examined by <sup>13</sup>C NMR spectroscopy. In all runs, there was exclusive formation of Et<sub>3</sub>Si(CH<sub>2</sub>)<sub>5</sub>CH<sub>2</sub>D (<5% deuterium incorporation at any other position by <sup>13</sup>C NMR), establishing that **6a,b** lie on the catalytic pathway and that *only* **6a,b** react with silane. Under catalytic conditions, then, **2** converts to **6** in a slow step (but nevertheless favored over its reaction with silane), which is followed by reaction of silane with **6** in a fast step. The concentration of **6** therefore remains low until silane is depleted to the point that consumption of **6** slows.

**D. Kinetic Studies.** The sequences of reactions established by NMR and labeling experiments predicts that the turnover rate, as governed by the rate-determining conversion of **2** to **6**, should show no dependence on silane or olefin concentration. Kinetics measurements are in agreement with this. As Table I indicates, with **[1]** = 0.01 M, an initial turnover rate of 0.5 min<sup>-1</sup> was found to be constant over a 5-fold range of both silane and olefin concentrations, consistent with isomerization of **2** to **6** being the turnover-limiting step. A typical kinetic plot of the turnover frequency is given in Figure 6, where the initial rate is based on the first 12 equiv of Et<sub>3</sub>Si(CH<sub>2</sub>)<sub>5</sub>CH<sub>3</sub> produced.

(21) Cracknell, R. B.; Orpen, A. G.; Spencer, J. L. *J. Chem. Soc., Chem. Commun.* 1986, 1005.

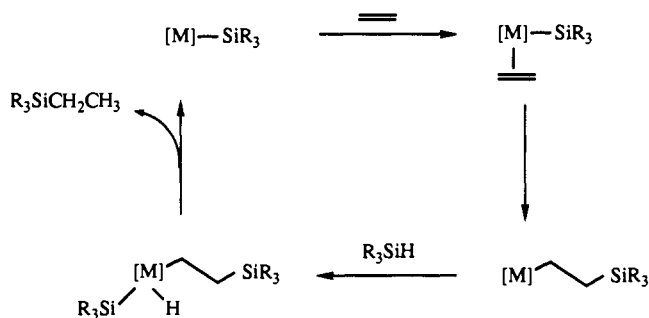
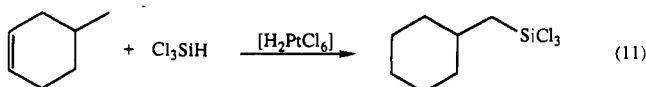


Figure 8. Proposed hydrosilation pathway for  $[M] = (\text{CO})_3\text{Co}$ ,  $\text{CpRhEt}$ .

## Discussion

Consistent with all of the observations is the overall catalytic cycle depicted in Figure 7. The spectroscopic detection of intermediate **2** has provided direct evidence for a silyl migration mechanism operative in a catalytic hydrosilation pathway. In this regard, the present mechanism resembles that shown in Figure 8, proposed by Wrighton<sup>13</sup> for  $[M] = (\text{CO})_3\text{Co}$  and later by Perutz<sup>14</sup> for  $[M] = \text{CpRhEt}$ . The pathway shown in Figure 8 invokes oxidative addition of silane as a discrete step leading to either a  $\text{Co}(\text{III})$  or a  $\text{Rh}(\text{V})$  species. A comparable step in our system would require oxidative addition of silane at a cationic  $\text{Co}(\text{III})$  center to yield a cationic  $\text{Co}(\text{V})$  species. An attractive alternative mechanism for conversion of **6** to **7** is a  $\sigma$ -bond metathesis process. Such a metathesis reaction could occur in a concerted fashion or via an intermediate species in which  $\text{Et}_3\text{SiH}$  is coordinated in an  $\eta^2$  fashion<sup>22</sup> to the highly electrophilic  $\text{Co}(\text{III})$  alkyl complex **6**, thus avoiding a cationic  $\text{Co}(\text{V})$  species.

The turnover-limiting isomerization step is noteworthy. Olefin isomerization and deuterium label scrambling, resulting from reversible  $\beta$ -H elimination/migratory insertion sequences and recognized as a common feature of hydrosilation catalysts, has been taken as evidence supporting the Chalk-Harrod mechanism, where rapid reversible  $\beta$ -H elimination precedes irreversible alkylsilyl reductive elimination. That  $\beta$ -H elimination/migratory insertion sequences occur prior to Si-C bond formation has been firmly established in many systems, most notably those in which isomerized olefin is observed at early stages of catalysis,<sup>23</sup> and systems whose hydrosilation product could *only* arise after prior isomerization. Equation 11 exemplifies this latter category.<sup>24</sup> It



should be noted, however, that these observations alone do not constitute proof that the Chalk-Harrod mechanism is operative. Facile olefin isomerization followed, in irreversible steps, by silyl migration and alkyl hydride reductive elimination is a sequence that is also consistent with these observations. In contrast,  $\beta$ -H elimination and isomerization, without release of vinylsilane, has been shown to occur subsequent to Si-C bond formation in the present catalyst system. Thus, the co-occurrence of olefin isomerization and silyl migratory insertion steps in a hydrosilation catalytic pathway has been established.

## Experimental Section

**General.** Reactions were conducted under an atmosphere of dry, deoxygenated nitrogen using standard Schlenk line techniques or in a Vacuum Atmospheres drybox. Hexane was distilled from sodium benzophenone ketyl, and methylene chloride was distilled over  $\text{P}_2\text{O}_5$  under a nitrogen atmosphere, prior to use. 1-Hexene (Kodak),  $\text{Et}_3\text{SiH}$  (Petrarch), and chlorobenzene (Aldrich) were stored over 4-Å molecular sieves and subjected to three freeze-pump-thaw cycles prior to use.  $\text{Me}_3\text{SiCH}_2\text{CH}_2$ ,  $\text{Et}_3\text{SiCH}_2\text{CH}_2$ ,  $\text{Me}_3\text{SiCl}$  (Aldrich), and  $\text{LiAlD}_4$  (CIL)

were used as received.  $\text{CD}_2\text{Cl}_2$  and  $\text{C}_6\text{D}_6$  were vacuum distilled and stored over 4-Å molecular sieves under nitrogen. The synthesis of **1** has been described.<sup>20</sup> NMR spectra were recorded on a Varian XL-400 NMR spectrometer.  $^1\text{H}$  chemical shifts were referenced to residual protio solvent:  $\text{CDHCl}_3$ , 5.32 ppm;  $\text{C}_6\text{D}_6\text{H}$ , 7.15 ppm.  $^{13}\text{C}$  chemical shifts were referenced to  $^{13}\text{C}$  solvent signals:  $\text{CD}_2\text{Cl}_2$ , 55.8 ppm;  $\text{C}_6\text{D}_6$ , 128.0 ppm. Gas chromatography (GC) analyses were conducted on a Hewlett-Packard 5890 using flame-ionization detection and a 30-m fused silica column with DB-5 as the active phase.

**Hydrosilation Reactions.** Preparative-scale catalysis was conducted as follows. To a methylene chloride (30 mL) solution of **1** (140 mg, 0.116 mmol) were added 1-hexene (1.45 mL, 11.6 mmol, 100 equiv) and then  $\text{Et}_3\text{SiH}$  (1.85 mL, 11.6 mmol, 100 equiv). After being stirred for 20 h, the reaction mixture was exposed to air and passed through a short plug of alumina ( $4 \times 1$  cm). Evaporation of  $\text{CH}_2\text{Cl}_2$  under reduced pressure gave  $\text{Et}_3\text{Si}(\text{CH}_2)_5\text{CH}_3$  as a clear oil (1.74 g, 75%).  $^1\text{H}$  NMR ( $\text{C}_6\text{D}_6$ ): 1.32 (m, 8 H), 0.96 (m, 12 H), 0.55 ppm (m, 8 H).  $^{13}\text{C}$  NMR: 34.6 (t,  $J_{\text{CH}} = 125$  Hz), 32.6 (t,  $J_{\text{CH}} = 125$  Hz), 24.9 (t,  $J_{\text{CH}} = 125$  Hz), 23.6 (t,  $J_{\text{CH}} = 125$  Hz), 15.0 (q,  $J_{\text{CH}} = 124$  Hz), 12.3 (t,  $J_{\text{CH}} = 115$  Hz), 8.4 (q,  $J_{\text{CH}} = 125$  Hz), 4.3 ppm (t,  $J_{\text{CH}} = 117$  Hz).  $(\text{Et}_3\text{Si})_2\text{O}$  was identified by comparing  $^{13}\text{C}$  NMR signals ( $\text{C}_6\text{D}_6$ : 7.7, 7.3 ppm) with an authentic sample.

**$^1\text{H}$  NMR Studies of Catalyst Solutions.**  $^1\text{H}$  NMR spectra of working catalyst solutions were obtained by dissolving in a 5-mm NMR tube **1** (20 mg) in  $\text{CD}_2\text{Cl}_2$  (0.8 mL) and cooling the solution to  $-78^\circ\text{C}$ . Five equivalents each of 1-hexene (10  $\mu\text{L}$ ) and  $\text{Et}_3\text{SiH}$  (13  $\mu\text{L}$ ) were added via a syringe into the septum-capped tube. A  $^1\text{H}$  NMR spectrum recorded at  $-70^\circ\text{C}$  showed both unreacted **1** and upfield resonances assigned to **2**. Allowing the sample to stand at room temperature for 2 min followed by recooling to  $-70^\circ\text{C}$  yielded a solution that showed only **2**. Warming the probe to  $0^\circ\text{C}$  gave upfield signals for **2a** that were well-resolved:  $-1.45$  (ddd,  $J = 11.9, 6.9, 1.5$  Hz,  $\beta$ -H),  $-9.75$  ppm (m,  $\mu$ -H). A sample identical to the one described except that it contained 10 equiv (20  $\mu\text{L}$ ) of 1-hexene was prepared, and the progress of the reaction was monitored by  $^1\text{H}$  NMR spectroscopy. After 40 min at  $0^\circ\text{C}$ , the sample was re-cooled to  $-70^\circ\text{C}$ . The spectrum recorded at this temperature showed hydride signals from **5**,  $-13.2$  (d,  $J_{\text{HP}} = 36$  Hz),  $-12.9$  (m), and  $-11.9$  ppm (m), along with signals from **2** as a minor species. The presence of  $\text{Et}_3\text{SiH}$ , 1-hexene, and  $\text{Et}_3\text{Si}(\text{C}_6\text{H}_{13})$  complicated the downfield portion of the spectrum and hampered assignment of the remaining signals from **2a** and **5**.

**Synthesis of  $\text{Cp}^*(\text{P}(\text{OMe})_3)\text{Co}(\text{C}_2\text{H}_3\text{SiEt}_3)$  (**4a**).**  $\text{Cp}^*(\text{P}(\text{OMe})_3)\text{Co}(\text{C}_2\text{H}_3\text{Me})$  (150 mg, 0.42 mmol) and  $\text{Et}_3\text{SiCH}_2\text{CH}_2$  (0.38 mL, 2.1 mmol) were heated in hexane (5 mL) at  $55^\circ\text{C}$  for 1 h. The resulting deep red solution was concentrated to ca. 1 mL and applied to an alumina column ( $5 \times 2$  cm). Elution with hexane followed by evaporation of solvent under reduced pressure gave **4a** as an air-sensitive red oil (112 mg, 58%). A second band that eluted with hexane/ether (2:1) was identified as  $\text{Cp}^*(\text{P}(\text{OMe})_3)\text{Co}(\text{C}_2\text{H}_4)$  by  $^1\text{H}$  NMR spectroscopy; its formation presumably arose from desilylation of **4a** on alumina and accounted for lower yields of **4a**.  $^1\text{H}$  NMR ( $\text{C}_6\text{D}_6$ ): 3.26 (d, 9 H,  $J_{\text{HP}} = 10.8$  Hz,  $\text{P}(\text{OMe})_3$ ), 2.09 (dd, 1 H,  $J_{\text{HH}} = 11.3$  Hz,  $J_{\text{HP}} = 0.9$  Hz,  $J_{\text{HSi}} = 8.1$  Hz, *cis*- $\text{CH}_2$ ), 1.66 (d, 15 H,  $J_{\text{HP}} = 1.8$  Hz,  $\text{C}_5\text{Me}_5$ ), 1.61 (dd, 1 H,  $J_{\text{HH}} = 13.6$  Hz,  $J_{\text{HP}} = 10.7$  Hz, *trans*- $\text{CH}_2$ ), 1.32 (t, 9 H,  $J_{\text{HH}} = 8.0$  Hz,  $\text{SiCH}_2\text{CH}_3$ ), 0.79 (m, 6 H,  $\text{SiCH}_2\text{CH}_3$ ), 0.44 ppm (ddd, 1 H,  $J_{\text{HH}} = 13.6, 11.3$  Hz,  $J_{\text{HP}} = 2.9$  Hz,  $\text{HCSiEt}_3$ ).  $^{13}\text{C}$  NMR ( $\text{C}_6\text{D}_6$ ): 91.3 (d,  $J_{\text{CP}} = 3.1$  Hz,  $\text{C}_5\text{Me}_5$ ), 50.7 (d,  $J_{\text{CP}} = 5.2$  Hz,  $\text{P}(\text{OMe})_3$ ), 39.6 (d,  $J_{\text{CP}} = 10.6$  Hz,  $\text{CH}_2$ ), 27.3 (d,  $J_{\text{CP}} = 4.0$  Hz,  $\text{HCSiEt}_3$ ), 9.8 ( $\text{C}_5\text{Me}_5$ ), 8.7 ( $\text{SiCH}_2\text{CH}_3$ ), 6.5 ppm ( $\text{SiCH}_2\text{CH}_3$ ). Anal. Calcd for  $\text{C}_{21}\text{H}_{42}\text{CoO}_3\text{PSi}$ : C, 54.76; H, 9.19. Found: C, 55.08; H, 9.07.

**Synthesis of  $\text{Cp}^*(\text{P}(\text{OMe})_3)\text{Co}(\text{C}_2\text{H}_3\text{SiMe}_3)$  (**4b**).** Complex **4b** was prepared using the same procedure as for **4a**; the volatile  $\text{Me}_3\text{SiCH}_2\text{CH}_2$  could be removed under reduced pressure, making chromatography unnecessary. Complex **4b** was isolated as a dark red crystalline solid (79%).  $^1\text{H}$  NMR ( $\text{C}_6\text{D}_6$ ): 3.25 (d, 9 H,  $J_{\text{HP}} = 9.3$  Hz,  $\text{P}(\text{OMe})_3$ ), 2.10 (dd, 1 H,  $J_{\text{HH}} = 11.6$  Hz,  $J_{\text{HP}} = 0.8$  Hz,  $J_{\text{HSi}} = 8.4$  Hz, *cis*- $\text{CH}_2$ ), 1.67 (d, 15 H,  $J_{\text{HP}} = 1.8$  Hz,  $\text{C}_5\text{Me}_5$ ), 1.64 (dd, 1 H,  $J_{\text{HH}} = 13.2$  Hz,  $J_{\text{HP}} = 10.8$  Hz, *trans*- $\text{CH}_2$ ), 0.61 (ddd, 1 H,  $J_{\text{HH}} = 13.3, 11.6$  Hz,  $J_{\text{HP}} = 3.2$  Hz,  $\text{HCSiMe}_3$ ), 0.35 ppm (s, 9 H,  $\text{SiMe}_3$ ).  $^{13}\text{C}$  NMR ( $\text{C}_6\text{D}_6$ ): 91.3 (d,  $J_{\text{CP}} = 3.7$  Hz,  $\text{C}_5\text{Me}_5$ ), 51.0 (d,  $J_{\text{CP}} = 6.1$  Hz,  $\text{P}(\text{OMe})_3$ ), 38.9 (d,  $J_{\text{CP}} = 8.8$  Hz,  $\text{CH}_2$ ), 33.0 (br s,  $\text{HCSiMe}_3$ ), 9.9 ( $\text{C}_5\text{Me}_5$ ), 2.8 ppm ( $\text{SiMe}_3$ ).

**Generation and Spectroscopic Characterization of  $[\text{Cp}^*(\text{P}(\text{OMe})_3)\text{CoCH}_2\text{CH}(\text{SiR}_3)\text{-}\mu\text{-H}]^+ \text{BAR}_4'^-$  (**5**).** Two different methods were employed to generate **5**;  $^1\text{H}$  NMR spectroscopy confirmed that both methods led to the formation of the identical species. Method 1: To a  $\text{CD}_2\text{Cl}_2$  (1 mL) solution of **1** (20 mg) in a 5-mm NMR tube was added 10 equiv of trialkylvinylsilane.  $\text{H}_2$  was bubbled slowly through the reaction mixture for 30 min, and  $^1\text{H}$  NMR spectra were recorded. Method 2: A  $\text{CD}_2\text{Cl}_2$  (0.5 mL) solution of  $\text{H}(\text{OEt})_2^+ \text{BAR}_4'^-$  (1.2 equiv) was added to a  $\text{CD}_2\text{Cl}_2$  (0.5 mL) solution of **4** (40 mg) in a 5-mm NMR tube at

(22) Schubert, U. *Adv. Organomet. Chem.* **1990**, *30*, 151.

(23) See, for example: Oro, L. A.; Fernandez, M. J.; Estruelas, M. A.; Jamenez, M. S. *J. Mol. Catal.* **1986**, *37*, 151.

(24) Ryan, J. W.; Speier, J. L. *J. Am. Chem. Soc.* **1964**, *86*, 895.

-78 °C.  $^{13}\text{C}$  NMR spectra of samples prepared in this manner were recorded at -80 °C.  $[\text{Cp}^*(\text{P}(\text{OMe})_3)\text{CoCH}_2\text{CH}(\text{SiEt}_3)\text{-}\mu\text{-H}]^+ \text{BAR}'_4^-$  (**5a**)  $^1\text{H}$  NMR (0 °C): 3.65 (d, 9 H,  $J_{\text{HP}} = 11.6$  Hz,  $\text{P}(\text{OMe})_3$ ), 3.21 (m, 1 H,  $\text{CoCH}_2$ ), 1.64 (d, 15 H,  $J_{\text{HP}} = 1.9$  Hz,  $\text{C}_3\text{Me}_5$ ), 0.95 (m, 9 H,  $\text{SiCH}_2\text{CH}_3$ ), 0.50 (m, 6 H,  $\text{SiCH}_2\text{CH}_3$ ), -1.63 (m, 1 H,  $\text{CoCH}_2\text{CHSiEt}_3\text{-}\mu\text{-H}$ ), -10.40 ppm (m,  $\mu\text{-H}$ ).  $^{13}\text{C}$  NMR (-80 °C) 97.0 ( $\text{C}_3\text{Me}_5$ ), 52.8 (d,  $J_{\text{CP}} = 6.0$  Hz,  $\text{P}(\text{OMe})_3$ ), 35.0 (dt,  $J_{\text{CP}} = 13.6$  Hz,  $J_{\text{CH}} = 156$  Hz,  $\text{CoCH}_2$ ), 9.0 ( $\text{C}_3\text{Me}_5$ ), -24.4 ppm (dd,  $J_{\text{CH}} = 128$  Hz,  $J_{\text{C-}\mu\text{-H}} = 74$  Hz,  $\text{CoCH}_2\text{CHSiEt}_3\text{-}\mu\text{-H}$ ).  $[\text{Cp}^*(\text{P}(\text{OMe})_3)\text{CoCH}_2\text{CH}(\text{SiMe}_3)\text{-}\mu\text{-H}]^+ \text{BAR}'_4^-$  (**5b**)  $^1\text{H}$  NMR (0 °C): 3.65 (d, 9 H,  $J_{\text{HP}} = 11.0$  Hz,  $\text{P}(\text{OMe})_3$ ), 3.23 (m, 1 H,  $\text{CoCH}_2$ ), 1.65 (d, 15 H,  $J_{\text{HP}} = 1.9$  Hz,  $\text{C}_3\text{Me}_5$ ), 0.10 (s, 9 H,  $\text{SiMe}_3$ ), -1.63 (m, 1 H,  $\text{CoCH}_2\text{CHSiEt}_3\text{-}\mu\text{-H}$ ), -10.65 ppm (m,  $\mu\text{-H}$ ).  $^{13}\text{C}$  NMR (-80 °C): 97.0 ( $\text{C}_3\text{Me}_5$ ), 52.7 (d,  $J_{\text{CP}} = 6.0$  Hz,  $\text{P}(\text{OMe})_3$ ), 35.0 (d,  $J_{\text{CP}} = 13.6$  Hz,  $\text{CoCH}_2$ ), 9.8 ( $\text{C}_3\text{Me}_5$ ), -18.6 ppm ( $\text{CoCH}_2\text{CHSiMe}_3\text{-}\mu\text{-H}$ ).

**Labeling Study.**  $\text{Et}_3\text{SiD}$  was prepared by stirring  $\text{Et}_3\text{SiCl}$  (4.49 g, 29.8 mmol) and  $\text{LiAlD}_4$  (1.50 g, 35.8 mmol, 99 atom % D) in ether (20 mL) for 12 h. Addition of water (10 mL) was followed by extraction with ether and then drying the organic fraction over  $\text{MgSO}_4$ . Evaporation of the solvent under reduced pressure gave  $\text{Et}_3\text{SiD}$  (1.64 g, 47%). A  $^1\text{H}$  NMR spectrum of the labeled product showed  $\text{Et}_3\text{SiH}$  to be present in ca. 5% of total silane. To methylene chloride (3 mL) solutions of **1** (50 mg, 0.041 mmol) were added 1-hexene (1.0 mL, 8.2 mmol, 200 equiv) and  $\text{Et}_3\text{SiD}$  (solution A, 66  $\mu\text{L}$ , 10 equiv; solution B, 0.66 mL, 100 equiv). A 1-mL aliquot of solution B was quenched after 20 min, and the remainder of solution B and solution A were stirred for 12 h. After workup,  $^{13}\text{C}$  NMR spectra of the three samples were recorded.  $\text{Et}_3\text{Si}(\text{CH}_2)_5\text{CH}_2\text{D}$  was identified as the sole product (<5% deuterium incor-

poration at any other position). The  $^{13}\text{C}$  NMR spectrum of the labeled product was identical to that of its unlabeled analogue, except for the methyl resonance as indicated:  $\text{Et}_3\text{Si}(\text{CH}_2)_5\text{CH}_2\text{D}$ , 15.0 ppm (tt,  $J_{\text{CH}} = 124$  Hz,  $J_{\text{CD}} = 18$  Hz).

**Kinetics Studies. Measurement of Initial Turnover Rates as a Function of  $\text{Et}_3\text{SiH}$  and 1-Hexene Concentrations.** A typical run is given: A Schlenk tube was charged with **1** (50 mg, 0.41 mmol), 1-hexene (0.52 mL, 4.13 mmol, 100 equiv), dodecane (50  $\mu\text{L}$ ), and chlorobenzene (3.15 mL). To this well-stirred mixture was added quickly  $\text{Et}_3\text{SiH}$ , at which point timing of the reaction began. Aliquots taken at 2-min intervals were efficiently quenched by injecting them into vials containing a few milligrams of alumina and shaking vigorously. Twelve samples were taken in this manner, and each was analyzed by gas chromatography (oven temperature = 140 °C, head pressure = 22 psi). Rates were calculated by integration of the  $\text{Et}_3\text{Si}(\text{CH}_2)_5\text{CH}_3$  (retention time = 3.3 min) signal versus the dodecane standard (retention time = 4.2 min). For each run, the volume of chlorobenzene was adjusted to maintain a constant concentration of **1**. A sample kinetics plot is shown in Figure 6; others are available in the supplementary material.

**Acknowledgment** is made to Dr. N. Pienta for assistance in preparing turnover rate plots and to the National Institutes of Health (Grant GM 28938) for support of this work.

**Supplementary Material Available:** Plots of initial turnover rates for reactions of various concentrations of silane and 1-hexene at catalyst concentration = 0.01 M (4 pages). Ordering information is given on any current masthead page.

## Power-Variable Electrophilic Trifluoromethylating Agents. *S*-, *Se*-, and *Te*-(Trifluoromethyl)dibenzothio-, -seleno-, and -tellurophenium Salt System

Teruo Umemoto\*<sup>†</sup> and Sumi Ishihara<sup>†</sup>

Contribution from the Sagami Chemical Research Center, Nishi-Ohnuma 4-4-1, Sagamihara, Kanagawa, 229, Japan, and MEC Laboratory, Daikin Industries, Ltd., Miyukigaoka 3, Tsukuba, Ibaraki, 305, Japan. Received September 21, 1992

**Abstract:** *S*-, *Se*-, and *Te*-trifluoromethylated dibenzoheterocyclic onium salts, their derivatives, and related salts were synthesized by the direct fluorination of a mixture of 2-[(trifluoromethyl)thio- or -seleno]biphenyls and triflic acid ( $\text{TfOH}$ ) or  $\text{HBF}_4$  etherate, by treatment of the corresponding sulfoxides and selenoxides with  $\text{Tf}_2\text{O}$ , by a new type of tellurium activation of 2-[(trifluoromethyl)telluro]biphenyl with  $\text{Tf}_2\text{O}$  and  $(\text{CH}_3)_2\text{SO}$ , or by derivation from the onium salts obtained. Examination of reactivity indicated the trifluoromethyl heterocyclic salts to be greatly reactive compared to nonheterocyclic salts and indicated that this heterocyclic salt system serves as a source of widely applicable trifluoromethylating agents. Their capacity to function as such varied remarkably and increased in the order of  $\text{Te} < \text{Se} < \text{S}$  and 2,8-dialkyl  $<$  3,7-dialkyl  $<$  H  $<$  3- $\text{NO}_2$   $<$  3,7-di- $\text{NO}_2$ . For mixed heterocyclic salts, the orders differed, apparently being determined by the electron deficiency of the  $\text{CF}_3$  group due to the electron-withdrawing or -donating effects of chalcogens and ring substituents, rather than the inherent nature of the chalcogens. Because of this variation, it was possible to trifluoromethylate a wide range of nucleophilic substrates differing in reactivity: carbanions, activated aromatics, heteroaromatics, enol silyl ethers, enamines, phosphines, thiolate anions, and iodide anions. The reaction mechanism is discussed, and a bimolecular ionic substitution mechanism competing with a free  $\text{CF}_3$  radical chain mechanism is proposed. Thus, a new field, electrophilic trifluoromethylation, has been established by the present study.

### Introduction

A trifluoromethyl group has unique features,<sup>1</sup> such as high electronegativity, stability, and lipophilicity. Thus, trifluoromethylated organic compounds are becoming increasingly important for developing new or more effective medicines<sup>2</sup> and agricultural chemicals<sup>3</sup> and new materials such as liquid crystals.<sup>4</sup> However, the methods for introducing a trifluoromethyl group into an organic compound are still unsatisfactory.<sup>5</sup> Free radicals<sup>6</sup> and nucleophilic trifluoromethylations<sup>7</sup> have been studied extensively and utilized for preparing trifluoromethylated compounds.

Electrophilic trifluoromethylation, however, has yet to be developed.<sup>5a,b</sup> This is because a trifluoromethyl cation is quite

(1) (a) *Organic Fluorine Chemistry*; Sheppard, W. A., Sharts, C. M., Eds.; Benjamin Inc.: New York, 1969. (b) Chambers, R. D. *Fluorine in Organic Chemistry*; A Wiley-Interscience Publication, John Wiley & Sons: New York, 1973. (c) Ishikawa, N.; Kobayashi, Y. *Fusso no Kagobutu*; Kodansha Ltd.: Tokyo, 1979.

(2) (a) *Biomedical Aspects of Fluorine Chemistry*, Filler, R., Kobayashi, Y., Eds.; Kodansha Ltd.: Tokyo, 1982. (b) Kumadaki, I. *J. Synth. Org. Chem., Jpn.* 1984, 42, 786. (c) Welch, J. T.; Eswarakrishnan, S. *Fluorine in Bioorganic Chemistry*; A Wiley-Interscience Publication, John Wiley & Sons, Inc.: New York, 1991.

<sup>†</sup> Present address: MEC Laboratory, Daikin Industries, Ltd.